Geophys. J. Int. (2013) doi: 10.1093/gji/ggt330
Geophysical Journal International Advance Access published September 11, 2013

Spatial and temporal forecasting of large earthquakes in a spring-block model of a fault

L. E. Aragón and E. A. Jagla
Centro Atómico Bariloche and Instituto Balseiro, Comisión Nacional de Energía Atómica, 8400 *Bariloche, Argentina. E-mail: aragon_l@hotmail.com*

Accepted 2013 August 16. Received 2013 August 13; in original form 2012 October 10

SUMMARY

We study a recently proposed statistical physics model of earthquake dynamics that includes stress relaxation in the plates as a fundamental ingredient. The model is known to reproduce many realistic features of seismic phenomena, such as: the Gutenberg–Richter law for the event size distribution, the Omori law for aftershocks and an overall velocity-weakening dependence of the average friction force. Here, we analyse the dynamics of the model in detail, in order to investigate to what extent the occurrence of large events in the model can be anticipated. We systematically find that large events occur in fault patches where strain accumulation has exceeded some threshold value. The spatial extent of these patches (which correlate with the magnitude of forthcoming events) can be calculated if the strain state of the system is supposed to be known. In addition, we find that some large events are preceded by well-defined precursor activity. This allows, in a fraction of cases, to complement the forecast of magnitude and spatial location, with a sensible prediction of time of occurrence. Although our work is exclusively limited to the numerical model analysed, we argue that it gives new breath to earthquake forecast techniques that combine the historical analysis of seismic activity with a search of appropriate precursor activity.

Key words: Time-series analysis; Spatial analysis; Earthquake dynamics; Earthquake interaction, forecasting, and prediction; Computational seismology; Statistical seismology.

1 INTRODUCTION

Earthquake prediction, in the sense of anticipating the occurrence of potentially large and destructive earthquakes, would certainly have an enormous practical importance. However, the possibility to predict earthquakes is still a most debated matter between specialists (Geller *et al.* 1997; Wyss 1997; Nature Debates 1999; Hough 2010; Jordan & Jones 2011; Crampin 2012; Eberhard *et al.* 2012). Attempts to predict earthquakes have focused on many different indicators that might inform about the future occurrence of a large earthquake. In this work, a forecast procedure is based exclusively in the analysis of mechanical properties of the Earth's crust, mainly on previous seismic activity and on the stress state of the plates.

Two important questions appear when we consider the possibility of earthquake prediction. Do we have, or eventually can have access to the variables that define the state of the system with enough precision to allow for a sensible prediction? and Do we have the evolution equations of the system that have to be solved in order to obtain the state of the system in a future time, if this state is known at present? It would be too speculative to try to answer these questions for a realistic case of earthquake prediction. Instead, we will focus on the possibility to predict the occurrence of events in a well-defined model of the seismic activity of a single planar fault. In this case, the answer to the second question is immediately affirmative, as we certainly know the equations that define the model. Regarding the first question, we will test on the model a forecast protocol that assumes some partial knowledge of the state of the system at a given time, and based on this information, tries to anticipate the occurrence of large events in the near future.

The issue of predictability in dynamic systems is too broad to make here even a succinct description (in this respect, see Boffetta *et al.* 2002). Restricting to seismic phenomena, forecasting procedures have been proposed for a variety of models. In particular, predictability in discrete, single-fault systems has been analysed from different aspects. For example, Kawamura *et al.* (2012) described the nucleation process as a precursor phenomenon, Ramos (2010) used the critical properties of temporal states to identify upcoming large earthquakes, Anghel *et al.* (2004) discussed how the different scales of motion involved in the dynamics of surface deformations impact predictability, Pelletier (2000) monitored the cumulative Benioff strain release that precede large earthquakes in spring-block models and Eneva & Ben-Zion (1997) and Shaw *et al.* (1992) identified particular clusters of events prior to large earthquakes.

It may be worth to analyse the effectiveness of a forecast procedure in our model, since it not only displays many realistic features of earthquakes and rock friction experiments (Section 3.2), but also incorporates relaxation effects in a consistent manner (Jagla 2010;

Jagla & Kolton 2010). Here, we show that a combination of strategies that have been followed in actual cases is useful to anticipate the occurrence of large events. Finally, we will argue that the results obtained within the context of this model give a reasonable hope that useful predictions may eventually be possible in a realistic context of actual seismicity.

The paper is organized as follows. In Section 2, we review some predictability methods proposed elsewhere. In Section 3, we describe the spring-block model which we used for simulating the dynamics of the tectonic plates as a statistical mechanic process. In Section 4, we discuss the possibility to anticipate the occurrence of large events in the model. Finally, in Section 5, we briefly summarize the results and discuss their potential applicability to actual earthquakes.

2 PREDICTION METHODS

Panakkat & Adeli (2008) presented a review of the work done in earthquake forecast in the past 20 yr. They classified the methods in two groups, one focused on a historical analysis of earthquakes and the other based on an analysis of earthquake precursors. This classification mostly matches the one made by the International Commission on Earthquake Forecasting for Civil Protection (ICEF) who distinguishes two approaches in the research of earthquake predictability (Jordan *et al.* 2011). On one side, they describe long-term, time-dependent forecasting models and on the other side, the analysis based on earthquake precursors. We give now a brief summary of both strategies.

2.1 Historical analysis and the seismic gap

Historical methods make an analysis of the earthquakes that occurred in some geographical region, generally during a period of time from 10 to 100 yr. They are useful to understand the behaviour of seismic areas in the long run. Among them, there are models of spatial predictability which are based on the idea that the occurrence of earthquakes is a statistical recurrent phenomenon. They consider different hypotheses about the spatial distribution of earthquakes in order to identify a 'domain of increased probability'. For a detailed explanation and examples of these models, refer to Zechar & Jordan (2008), Nanjo (2010) and Shcherbakov *et al.* (2010).

Other historical methods are based on the elastic rebound theory proposed by Reid (1911) which states that the next earthquake is likely to occur when enough strain has been accumulated since the last event. These methods assume that large earthquakes in a fault occur in quasi-periodic cycles, and try to estimate when the next one will be generated, at the end of the current cycle. Closely related to the methods based on the existence of a seismic cycle, there are others that identify the areas where there is more accumulated strain and the next large earthquake is expected to occur ('seismic gaps'). These are the fault patches that have been completely locked for long periods, or that have accrued less displacement than expected from the long-term tectonic motion (i.e. they have a 'slip deficit'). Originally, the seismic gaps were exclusively determined by knowing the seismic history of a certain region. More recently, geodetic technologies such as 'Global Navigation Satellite Systems' (GNSS) and 'Interferometric Synthetic Aperture Radar' (InSAR) have been applied to complement this information with more precise measurements of the plate displacements.

The last two great subduction earthquakes took place in fault patches previously identified as seismic gaps. Ruegg *et al.* (2009) reported that in the region between Constitución and Concepción in Chile, there had been over 175 yr with no release of the strain accumulated by the convergence of the Nazca and South American plates. They commented that in the worst-case scenario, the accumulated displacement corresponds to more than 10 m, or equivalently to that of an earthquake of magnitude between 8 and 8.5. On 2010 February 27 an 8.8 magnitude earthquake took place in the region specified by Ruegg *et al.* (Madariaga *et al.* 2010). Nishimura *et al.* (2004) identified two areas between the North American and Pacific plates in NE Japan with the largest interplate coupling. One of them (the Miyagi-Oki region at 38°N, 142.5°E) presented the maximum strain accumulation. They emphasized the potential danger of this locked area and estimated that it could generate an earthquake of magnitude 7.5. On 2011 March 9, a 7.5 magnitude earthquake occurred at 38.4°N, 142.8°E. Two days later, a magnitude 9 earthquake took place at 38.3°N, 142.4°E.

These two examples give evidence that historical methods may serve to identify potentially dangerous areas where large earthquakes are likely to occur in the future.

2.2 Precursors and seismicity patterns

Many efforts to predict earthquakes are based on detecting and analysing precursor signals which anticipate a big event, generally in a timescale of months or days. Among them there are methods based on detecting signals which are indirectly related to the seismic phenomena (such as electromagnetic waves, radon in the air and water level anomalies). On the other hand, there are methods based on detecting patterns in the variables directly linked to the system's mechanics: fluid-rock deformation (Crampin *et al.* 2008), fault creep, abrupt stress changes in the crust (Li *et al.* 2003) and patterns in the occurrence of past earthquakes (Kanamori 1981; Wyss *et al.* 1999). The ICEF has recently concluded that the search for precursors that ensure with high probability that a target event will occur in a specific subdomain has so far been unsuccessful. Nevertheless, they emphasize that the observation of physical precursors can improve the methods for probabilistic forecasting, meaning that their observation might inform about the increasing probability of an upcoming event (Jordan *et al.* 2011).

Among the precursor phenomena just mentioned, seismicity patterns are the most frequently reported, probably because they involve examining earthquake catalogues which constitute the largest data set that may be monitored for evidence of precursors (Scholz 2002). They include precursory swarms (Rhoades 2010), seismic quiescence, doughnut pattern, foreshocks (Lippiello *et al.* 2012) and empirical pattern recognition (Kossobokov 2006). These methods compute different metrics calculated from past seismic activity and identify patterns that will anticipate larger events. Two important aspects should be considered regarding these methods: the identification of precursory seismicity patterns depends on some parameters that must be empirically adjusted, and the values of these parameters depend on the seismic region considered.

An example of this last kind of method is called 'Reverse tracing of precursors (RTP)' (Keilis-Borok *et al.* 2004; Shebalin *et al.* 2006). It is based on considering precursors in inverse order of appearance. First, chains which reflect the candidates in the short term are detected. These chains are basically a sequence of small earthquakes that occur spatially and temporally grouped. Secondly, intermediate-term precursors are searched in the vicinity of each chain. If found, a short-term alarm is declared. The advantage of using these chains is that it limits the search of intermediate-term

precursors exclusively to the region where the short-term precursors took place. The forecasting skills of this method is still in doubt (Zechar & Zhuang 2010), but longer monitoring periods with more target events are needed to complete the statistical analysis (Molchan & Romashkova 2011).

3 STATISTICAL MODELLING OF SEISMIC PHENOMENA

The modelling on any complex phenomenon necessarily implies neglecting many variables that are supposed not to be crucial for the description, and concentrating in others that are supposed to be the most relevant for a description as accurate as possible. It is the matching between the output of the model and that from the actual process what makes the modelling successful. It is natural to consider that, if a model reproduces a number of non-trivial features of the actual phenomenon, then a relatively fair understanding of the process has been achieved.

Remarkable features of seismic phenomena have been simulated when the complex dynamics of the tectonic plates is described by very simplified statistical mechanic processes (Sornette & Werner 2009; Kawamura *et al.* 2012). The pioneer model of Burridge and Knopoff (BK, Burridge & Knopoff 1967; Carlson *et al.* 1994) focuses on one planar fault by considering a system of blocks and springs (representing portions of the plates and its elastic properties) that are forced to slide onto an underlying rigid surface (see Fig. 1). Earthquakes in the model are seen as a cascade of instabilities of this dynamic system governed by the collective behaviour of its multiple degrees of freedom. Based on the BK model, Olami *et al.* (1992) presented these ideas in the form of a cellular automaton [OFC (Olami-Feder-Christensen) model], where the dynamics is defined as a list of rules, being simple enough to be simulated very efficiently (Grassberger 1994). Since then, the OFC model has become one of the paradigms of simulation of seismic activity (Kawamura *et al.* 2012).

3.1 The OFC model

The OFC model considers a set of real-valued variables u_i, where i indicates the position in a 2-D lattice. u_i is interpreted as the friction force that a rigid substrate exerts on a solid block at position i, and represents the local stress between the sliding plates (see Fig. 1). The system is driven by uniformly increasing the values of u_i with time at a rate V, simulating the tectonic loading of the plates. Every time one of the variables u_i goes beyond a maximum threshold (ordinarily uniform across the system), the block i is displaced, and this produces a rearrangement of the stresses: the local stress u_i is reduced a quantity Δu, and the stress on the neighbour sites j increase according to $u_j \rightarrow u_j + \alpha \Delta u$ (see Fig. 2). Usually, the value of Δu is taken equal to u_i itself, so the local value of the stress is reduced to zero. The value of α can vary between 0 and $\alpha_c \equiv 1/z$, z being the number of neighbours in the lattice. We will refer only to the case of a square lattice, so $z = 4$, $\alpha_c = 1/4$. A discharge can produce the overcome of the maximum local stress

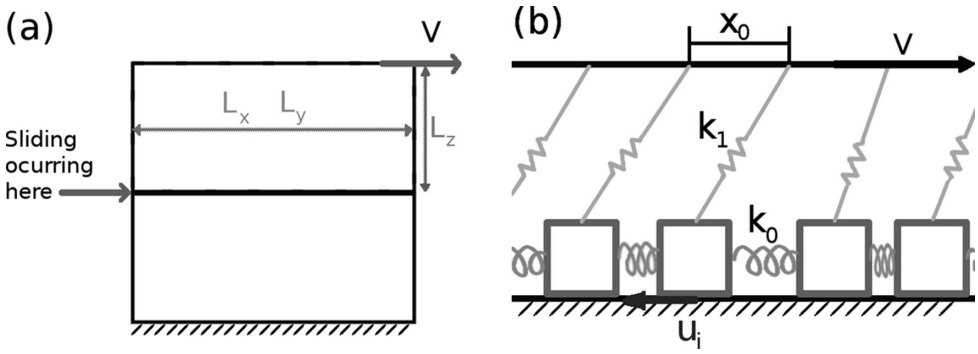

Figure 1. A sketch of the sliding situation that we are studying. (a) Two solid blocks slide against each other due to a constant driving between the top and bottom planes. Their relative velocity is V. Dimensions of the blocks are L_x, L_y in the sliding plane and L_z perpendicularly to it. (b) The solids in (a) are replaced by a rigid surface and an array of small blocks joined by springs with constant k_0 and separated a nominal distance x_0. Driving acts on each block through a spring of stiffness k_1 (Aragón *et al.* 2012).

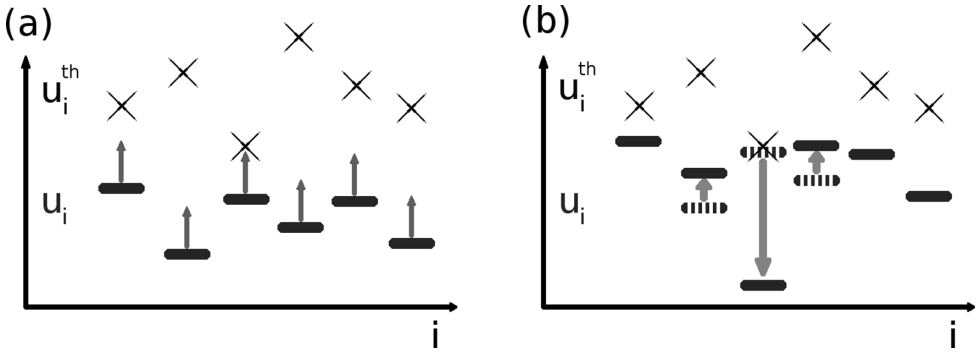

Figure 2. A sketch of the OFC model's dynamics with variable thresholds. The values of friction forces u_i and maximum forces u_i^{th} at each site are shown. (a) During the quasi-static evolution of the system, as driving proceeds, the friction forces increase uniformly (indicated by the arrows). (b) The system becomes out of equilibrium as one u_i reaches the local threshold u_i^{th} and evolves instantaneously. The automata prescription is shown: u_i decreases a quantity Δu (long downward arrow), and the neighbours increase their u values a fraction $\alpha \Delta u$ (short upward arrows). Note that a cascade can be generated and will be identified with an individual quake (Aragón *et al.* 2012).

on one, or more than one neighbour, and so on, generating a cascade, or avalanche. This cascade is called an event, and is identified with an individual earthquake (note that the complete cascade is assumed to occur at constant time, namely, earthquakes are instantaneous). The total number of sites involved in a given avalanche is naturally identified with the area A of the event. The non-dimensional seismic moment S is calculated as the sum of the block displacements over the entire rupture area, and the magnitude of the event is defined (up to an additive constant) as $M = \frac{2}{3}\log_{10} S$ (Hergarten 2002, p. 145; Scholz 2002).

The decrease of u_i by some quantity Δu when block i becomes unstable implies that its position (that we call h_i) increases by an amount δ, given by $\delta = \Delta u/(4k_0 + k_1)$, where k_0 is the stiffness of the springs that interconnect the blocks and k_1 is the stiffness of the springs that pull the blocks at velocity V. k_0 and k_1 are proportional to Ex_0 and Ex_0^2/L_z, respectively, where E is a typical elastic constant of the bulk material, x_0 is the nominal distance between discrete blocks and L_z is the thickness of the sliding plate (see Fig. 1). Thus, it can be seen that $\alpha = \frac{k_0}{4k_0+k_1} = \frac{1}{4+x_0/L_z}$, which is independent of the elastic constant of the plates.

The value of α determines the degree of stress transfer in the system, and the limit $\alpha \to \alpha_c = \frac{1}{4}$ is usually referred to as the conservative case, where the excess stress of an unstable site is fully redistributed to its nearest neighbours (note that this limit corresponds to $k_1/k_0 \to 0$ in our case). The model is dissipative for any value of α; there is a finite average friction force in the system (which is the average force on the k_1 springs) that implies a dissipation of energy as the driving proceeds.

We note that from the values of u_i we can reconstruct the local strain of the plates w_i [defined as $w_i \equiv (Vt - h_i)$] by solving the discrete differential equation that ensures mechanical equilibrium of forces during the quasi-static evolution of the system:

$$u_i = k_1 w_i - k_0 \left(\nabla^2 w\right)_i, \tag{1}$$

where ∇^2 is the discrete Laplacian on the underlying square lattice, namely $(\nabla^2 w)_i \equiv (\sum_j w_j - 4w_i)$, where j stands for the four neighbour sites to site i. Either u or w will be used to characterize the mechanical state of the system.

The OFC model generates a broad distribution of event sizes, even if the model itself does not contain such a distribution in its definition, namely, this distribution is dynamically generated. However, other robust features of seismic phenomena are not reproduced by the model, and this led us to consider some variations of the OFC model Untitled Document 1 (which are motivated by the physics of seismic phenomena) to produce more realistic results.

3.2 The modified OFC model

Having in mind a realistic situation of a heterogeneous fault, with the constitutive materials having different properties at different positions, it becomes natural to consider a case in which the threshold values for the variables u_i are not constant but have some spatial variation. This is the first modification we have introduced onto the OFC model. Namely, the values of the local thresholds will be called $u_i^{\rm th}$, and we draw them from a Gaussian distribution centred at 1 with standard deviation 0.6. These values (as well as stresses themselves) are not truncated at 0, since the results do not depend on the mean value of $u_i^{\rm th}$. We can always choose a larger mean, and strictly positive values of $u_i^{\rm th}$. Each time u_i exceeds the local threshold $u_i^{\rm th}$, u_i is updated to a new value. We use the update rule $u_i \to u_i - \Delta u$, using a fixed value of Δu, that is, we implement a prescription of constant elementary stress drop (see Fig. 2). Every time u_i is updated, a new value is assigned to the local threshold $u_i^{\rm th}$, taken from its original random distribution. This prescription is justified on the same physical arguments as before, since the sliding pieces can reasonably be thought as finding different maximum strengths as sliding proceeds.

The second and crucial modification we made on the OFC model is the introduction of internal relaxation effects. We will not repeat here the arguments that justify this introduction, which can be read in the original publications (Jagla 2010; Jagla & Kolton 2010), but let us just mention the following fact that points to the necessity of these effects: In the OFC model, a sudden stop of the tectonic loading makes all seismic activity to cease at once. This is unrealistic, as for instance the processes that trigger aftershocks after a main event depend on the rearrangements that occur in the fault network after the main shock, and are not directly related to tectonic loading. In other words, dynamic effects within the faults should be taken into account in order to have a realistic description of the seismic process. This is what we did by introducing the internal relaxation mechanism. The actual implementation prescribes that the evolution of the variables u_i between avalanches obeys

$$\frac{{\rm d}u_i}{{\rm d}t} = R\left(\nabla^2 u\right)_i + k_1 V. \tag{2}$$

The $k_1 V$ term represents the external loading and can be easily deduced from eq. (1) and recalling that $\frac{{\rm d}w_i}{{\rm d}t} = V$. The R term tends to make the values of u_i progressively more uniform in the system, reducing its total energy. In (Jagla & Kolton 2010 and Jagla 2010), the use of this new term is justified with more detail. Throughout the paper, we will be working with dimensionless units, measuring stresses in units of Δu, spatial distances in unit of x_0, strains in units of δ, time in units of $\frac{\Delta u}{k_1 V}$ and the strength of the relaxation effect R in units of $\frac{k_1 V}{\Delta u}$.

The two modifications just described make the results of the simulations to be much more realistic in several respects (see Jagla 2010; Jagla & Kolton 2010); Aragón *et al.* (2012) for examples of the results that are obtained:

(1) The spatial and temporal correlation of events is now comparable to real ones, in particular, aftershock sequences obeying the Omori law (Omori 1894) are obtained;

(2) The distribution of avalanche sizes has a Gutenberg–Richter form, with an exponent b very close to actually observed values ($b \sim 1$);

(3) The friction properties derived from the model reproduce non-trivial results such as velocity weakening or the stress peak in experiments of slip-stop-slip;

(4) Contrary to the $R = 0$ case, events of size comparable to the system size persist in the macroscopic limit ($\alpha \to 0.25, L_z \to \infty$);

(5) The temporal evolution of seismic activity supports the concept of a 'seismic cycle'.

It is worth mentioning that as long as R is larger than some minimum value, all these results are obtained irrespective of the precise value of R.

We will comment on a few fundamental differences between the OFC model and the modified implementation used here. The OFC model is typically simulated using open boundary conditions; otherwise, the spatial homogeneity generated by the use of periodic conditions induces a strong global synchronization in the model. As explained in Jagla (2010), in our model with non-uniform thresholds, the differences in bulk quantities calculated using open or periodic boundary conditions become negligible when system size is large enough. Even though there are not periodic boundary

conditions in actual faults, we work with periodic boundary conditions mostly to take advantage of spectral techniques that we used to temporally evolve (eq. 2). The system size is taken large enough, such that the largest events observed fit well into the system, and no system size dependences of the results are observed if size is further increased. It must also be taken into account that the value of the parameter α has qualitatively different effects in this model and in the original 'OFC' model. In the OFC model, the value of α determines the slope of the Gutenberg-Richter law, and the maximum size of the avalanches is only bounded by the system size, whereas here, the exponent b of the size distribution does not change with α, and the maximum avalanche sizes gets larger without limit as $\alpha \to 0.25$ (Jagla 2010). We always use values of α and system sizes such that the maximum avalanche area is smaller than the system size.

4 IMPLEMENTATION OF A FORECASTING PROTOCOL IN THE MODEL

Our aim is to analyse to what extent the occurrence of large events during the time evolution of the model can be anticipated. To address this point, we need to be more precise in a few different aspects.

The first one is to clearly define what we call a large event. In Fig. 3, we show a typical temporal sequence of events in the model at two different timescales. In the bottom panels, we observe a systematic pattern of steady increase in the average stress in the system $\overline{u}_i$, followed by abrupt drops. In Aragón *et al.* (2012), we interpret this cycle of a smooth stress increase and sudden stress decrease as the manifestation in our model of a 'seismic cycle' (Scholz 2002). We would like to predict the imminent occurrence of these abrupt drops of stress in the system, which correlate with the largest individual events in the model. However, a more careful observation of the sequence of events reveal that in most cases, what looks at first sight as a single drop of stress, is composed by many contributions from clusters of events that occur very close in time. Our scheme will focus on predicting these tight clusters (indicated by the double arrows in the lower right panel of Fig. 3), so we will redefine from now on an 'event' as the whole cluster of quakes that generate this composite stress drop. To be precise, we will consider that an event starts when a first quake of magnitude larger than 1.85 occurs, and ends if no quake of magnitude larger than 1.85 occurs within a time 0.001. We can mention that in actual seismicity, large events also occur within 'clusters', typically of one or more main shocks, and a large number of aftershocks. However, the largest main shock takes typically as much us 90 per cent of the total seismic moment of the cluster, so neglecting the rest of the cluster produces only a minor error. In our case, it is typically observed that the cluster is formed by few different events with a relatively large contribution to the total released seismic moment, so it is important to consider the whole sequence. We think this slightly unrealistic feature of our model is due to the fact that we do not consider long-range elastic interactions, or inertia effects in a realistic way.

The second point we have to consider, is that any sensible forecasting procedure we propose, must be based on a limited number of variables characterizing the state of the system. The necessity of this is absolutely clear for the actual case of real seismicity, in which the system is a piece of the Earth's crust, as it is hopeless to expect to have access to a full set of variables that characterize precisely its state at every spatial scale. Typically, we can expect to have access to some coarse-grained variables that describe the average elastic state of the crust. Using the same philosophy, we will not set up a forecast scheme for our model on the basis of the knowledge of every microscopic variable. In our model, there are a number of variables that are well defined at any moment, namely the local stresses u_i (which determine the local strains w_i; see eq. (1)) and the local thresholds $u_i^{\rm th}$. Also, upon a deterministic evolution of u_i, when an avalanche occurs, the new thresholds are generated in a stochastic manner. Among all these variables, the thresholds are certainly the most difficult to monitor in a realistic situation. Our forecasting scheme will assume that we do not have any knowledge on the values of $u_i^{\rm th}$. With respect to the values of u_i (or w_i), we will take as a starting point that we have a complete knowledge of these variables. It is out of question that this is not realistic for actual seismicity at present. However, modern experimental techniques based on GNSS monitoring allow to observe spatial variations of the strain distributions caused by individual earthquakes. In addition, as we show in Appendix A, the form of u_i and w_i can be recovered for our model if we have access to a sufficiently detailed record of the local slips caused by previous earthquakes. A forecast scheme based on the knowledge of only a part of the variables that are necessary to conduct a full numerical evolution of the model cannot be fully accurate, but will have (in the best case) only a statistical significance.

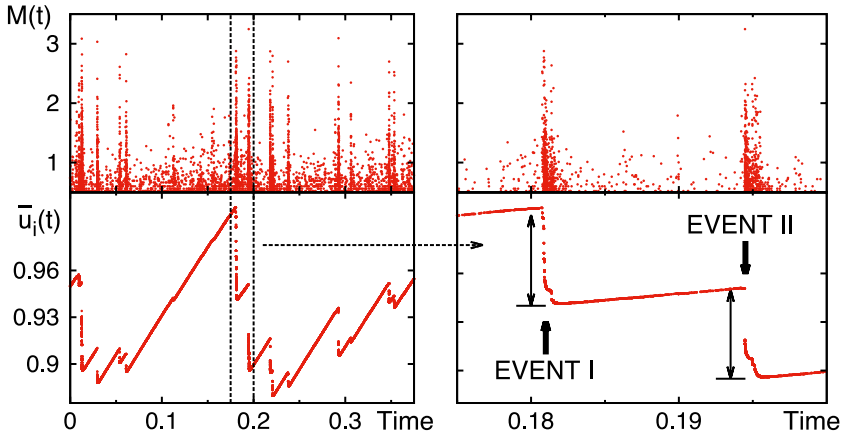

Figure 3. Temporal event sequence characterized by the magnitude of the events M (top panels) and average stress in the system $\overline{u}_i$ (bottom panels). The dashed vertical lines in the left-hand panels indicate the temporal interval shown in the right-hand panels, where two target events are shown in detail. The stress drop of each event is indicated by double arrows. Results correspond to a system of 256×256, with $R = 1000$ and $\alpha = 0.243$.

However, if the occurrence of large earthquakes within some limited time window can be forecast in a significant number of cases, this will have valuable practical implications.

The third important consideration is to note that a potentially useful forecast should combine both a precise anticipation of geographical location and magnitude of a large forthcoming event and a statistically significant information about the time of occurrence of the event.

We have developed a procedure for our model that combines the methods summarized in Sections 2.1 and 2.2. The information provided by the distribution of local strain allows to find fault patches that are 'overdue' with respect to the average displacement of the plates. The extent of these patches informs us of what the maximum magnitude is of an event that will eventually occur there. This is a procedure that follows closely the strategy of Section 2.1. Once overdue fault patches are identified, we look for the appearance of typical precursor activity in it, in a qualitatively similar way to the procedure of Section 2.2. We find that when typical precursor activity occurs within high-strain zones, there is some probability that a large event will be triggered within a limited time period. If however, the same kind of activity is detected in spatial locations that are not overdue, this will not typically produce a large event in the near future.

4.1 High-strain zones

The idea presented in Section 2.1 that large earthquakes occur in large spatial seismic gaps is well realized in our model. We present some results corresponding to a system of 256×256, with $R = 1000$ and $\alpha = 0.243$. Fig. 4(a) shows the spatial distribution of strain w_i in the system a small time before the event indicated in Fig. 3 as 'I'. In Fig. 4(a), it is apparent that there are regions with particularly large values of strain, namely, a large seismic gap. Fig. 4(b) is the strain distribution after some time, once event I has occurred. Figs 4(c) and (d) show, as another example, the strain distributions before and after event II in Fig. 3. We see that the regions spanned by the events correspond approximately to overdue fault patches in which the strain was larger than some threshold value, which for the present parameters of the model was found to be around 36.5 (in units of δ). In the absence of any other guidance, we choose the threshold value of the strain distribution to be (from test runs) such as to match the area spanned by the events once they actually occur. Smaller values of the threshold strain would correspond to contour areas much bigger than the areas of the target events, while larger values would have the opposite effect. This correlation was observed systematically for many large events, and shows that if we know the strain distribution in the system, an identification of the spatial extent of forthcoming events can be made before they actually occur. This is the same kind of strategy discussed in Section 2.1, and corresponds to identifying the fault patches in which the slip deficit is particularly large.

In Figs 4(b) and (c), the effect of internal relaxation can be appreciated. In Fig. 4(b), the dark region affected by the recent event presents some bright spikes which correspond to blocks with high-strain values. These spikes tend to disappear as the strain becomes more uniform due to relaxation. This is a direct effect produced by the R-proportional term in eq. (2) and represents the slow rearrangements of the sliding plates which tend to minimize the system's total energy. This relaxation effect is also responsible for the appearance of aftershocks in the system.

Even though, in the model used in this work, we can clearly identify that large events rupture mainly the high-strain patches and

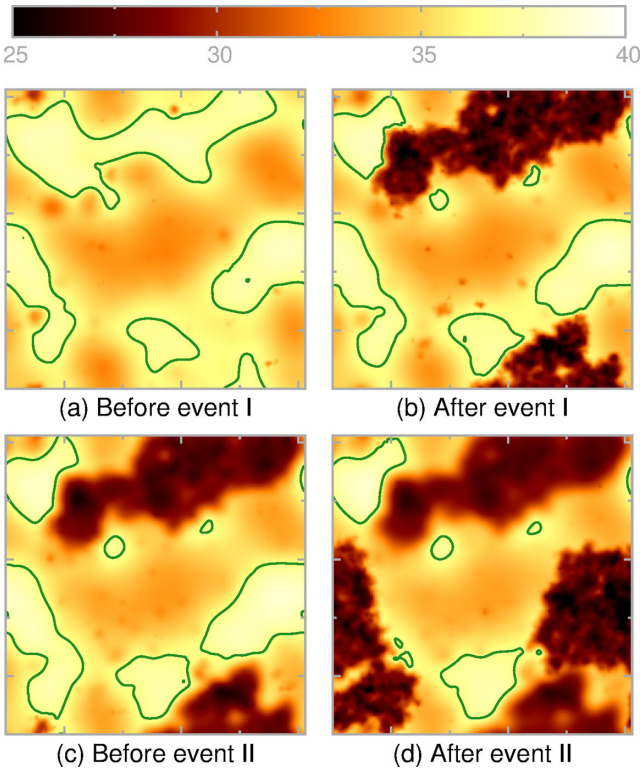

Figure 4. Spatial distribution of strain w_i in the x-y plane of a fault (see Fig. 1) modelled by a numerical lattice of 256×256 elemental blocks, with $R = 1000$, $\alpha = 0.243$ and periodic boundary conditions. A brighter colour indicates a higher value of w_i. The maps shown correspond to the state of the system before and after event I (a and b) and event II (c and d) indicated in Fig. 3. The slip areas of these events are clearly identified as the regions in which w_i is largely reduced. In this figure, contour lines are drawn at a particular value $w_i = 36.5$. It is observed that events tend to 'fill up' some of these contour lines, thus allowing the identification of 'overdue fault patches' where large events systematically occur.

the rupture is arrested by the low-strain patches, we emphasize that these are not persistent features, namely, the position of high-strain regions where events are most likely to occur changes along time, and in the long run the activity is homogeneous across the system. The actual existence of earthquakes that occur almost periodically in high-stress patches with almost the same rupture zone and epicentre (see, for instance, Kawamura *et al.* 2012) is a phenomenon that is associated to inhomogeneous features of a particular fault, which are not included in our scheme.

In Fig. 5(a), we plot the area of the events observed as a function of the area of the 'overdue fault patches' in which they occurred. An event is considered to occur inside a target region if its epicentre (first block moved) is within this region. On the vertical axis, at the left part of the figure, we also plot the area of events that do not take place inside overdue regions. It is straightforward to see that all events which have an area larger than a certain threshold (indicated by a horizontal dotted line) occur within overdue regions. This shows again that the spatial occurrence of large events can be anticipated very well. The plot also shows that given the area of an overdue region, we can establish an approximate upper bound for the area of the events which will occur there (indicated by the dashed line of slope 0.8). The correlation between expected and actually observed areas of the events can be translated to a corresponding expected/observed magnitude relation. In fact, the area of observed

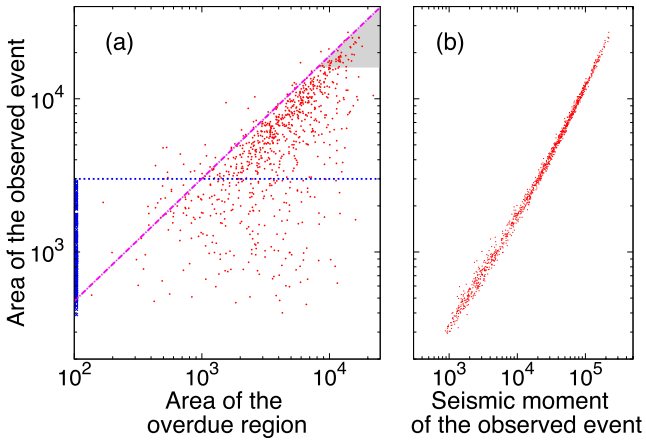

Figure 5. (a) Area of the observed events as a function of the area of the overdue patch. On the y-axis, at the left part of the figure, we also plot the area of events that do not take place in overdue patches, whose upper limit is indicated by the horizontal dotted line. The dashed line of slope 0.8 indicates the approximate upper bound for the area of the events which will occur in a given overdue patch. The shaded region correspond to target events with a minimum area $A_{\min} = 1.6 \times 10^4$. (b) Area of the observed events as a function on their corresponding seismic moment.

events correlate very well with the seismic moment S of the event as it can be seen from Fig. 5(b). It is then clear that if we would like to predict events larger than a certain size, or magnitude, they must have an area larger than a certain minimum $A_{\min}$. These events will be called target events and $A_{\min}$ defines the minimum size of the overdue regions which we will consider.

4.2 Precursor activity

The analysis of strain distribution provides an accurate determination of the maximum magnitude and location of large events that are likely to occur along the temporal evolution of the system. Remarkably, we find in our model a number of cases in which the occurrence of these large events can be anticipated by the detection of precursor activity in the spatial region of interest. This is the same idea we discussed in Section 2.2. In fact, in many cases it is observed in the model that some typical pattern of activity, in the form of a few comparatively small quakes that form what we call a 'chain', occurs shortly before the large event. Thus, this can be taken as a signal to declare an alarm for the possible occurrence of a large event in the immediate future. Particular clusters of events, both in real and synthetic catalogues, have been regarded as precursor activity in a number of works, for instance in Shaw *et al.* (1992), Eneva & Ben-Zion (1997), Baiesi (2006), Shebalin (2006) and Rhoades (2010).

To provide some practical examples, we have to define with more precision the concept of a chain. They are defined by linking quakes that occur closer to each other than some maximum space and time intervals. In principle, these intervals should depend on the magnitudes of the quakes that are considered (Baiesi & Paczuski 2004). If, for simplicity, we use fixed space and time intervals, we need to consider only quakes that are within a certain magnitude range $[M_1, M_2]$. We will say we have detected a chain when a number of linked quakes greater than some minimum $n_{\min}$ has been detected. The values of the maximum space and time interval for two quakes to be linked, the magnitude range and $n_{\min}$ are adjusting parameters that have to be tuned to obtain the best performance of the forecast algorithm.

Without attempting to optimize the parameters for the best possible performance, we use the following values for the detection of chains in our simulations: maximum time interval: 0.001; maximum spatial interval: 20 lattice units, magnitude range: $M_1 = 0.40$, $M_2 = 1.85$, $n_{\min}$: 9. M_2 was chosen to be as high as possible, while low enough so that a quake of this magnitude does not produce an appreciable drop in the mean stress of the system. The temporal and spatial intervals were chosen to be small enough so that linked quakes were not too common. We have verified that the results depend smoothly on these parameters. In principle, an optimization can be made to find the best set of parameters for the forecasting scheme. However, we will not proceed with this optimization here.

Many chains that fit this criterion occur in the system along the temporal evolution, but we will only concentrate on those (that we call 'precursor chains') localized within high-strain zones. Precursor chains may be associated to the foreshocks that are usually retrospectively identified once the upcoming big event has been observed. We note that the precise definition and identification of foreshocks in real and simulated seismicity is an active field of research (Helmstetter *et al.* 2004; Lippiello *et al.* 2012). In our case, the observation of a precursor chain is the signal that activates an alarm. The alarm indicates that there is an enhanced probability that an event of a maximum magnitude (given by the size of the overdue region in which the chain takes place) may occur in the near future. For practical reasons, this alarm is defined to be active during some time interval Δt. The value of Δt is a fitting parameter of the forecasting scheme. To evaluate the success of our algorithm, we will consider that a hit corresponds to a target event that starts in the target region within the interval Δt. Otherwise, it is a miss, and the alarm was a false alarm.

To present the results of the temporal forecast procedure, we note first that the effectiveness will strongly depend on the particular value of Δt used. Thus, we will show the results obtained as a function of the value of Δt. Two complementary quantities will be presented. One is the fraction η_1 of target events that occur within alarm periods, namely, the number of events that occur at times where the corresponding alarm was active $N_{\text{predicted}}$, divided by the total number of target events N_{total}: $\eta_1 = N_{\text{predicted}}/N_{\text{total}}$. Obviously, we want to maximize this number. However, this has to be done keeping the system on alarm as brief as possible. So the other variable we will present is the fraction η_2 of the total time that the system is on alarm. For a simulation of a duration T_{total}, if the system is in alarm during a time T_{alarm}, we have $\eta_2 = T_{\text{alarm}}/T_{\text{total}}$. In Fig. 6, the two numbers η_1 and η_2 are presented as a function of Δt for a minimum area of the target events $A_{\min} = 1.6 \times 10^4$ (shaded region in Fig. 5). In the present case, $N_{\text{total}} = 190$ and $T_{\text{total}} = 88.8$. We have checked that a further increase of T_{total} does not produce systematic changes in η_1 and η_2, only reduces statistical fluctuations.

The effectiveness of the forecast algorithm can be evaluated through the probability gain $\eta \equiv \eta_1/\eta_2$. In fact, η is the density of target events during periods of alarm, divided by this density at all times. A null prediction corresponds to $\eta = 1$. When $N_{\text{tot}} \to \infty$, any value above 1 reveals some degree of efficiency of the algorithm. The value of η is also plotted in Fig. 6. We see that we obtain systematically values of η above one, up to values close to 14 when Δt is properly adjusted. In other words, we are able to identify some periods of time following the observation of precursor chains, in which the probability to observe target events is about 14 times larger than the average probability. To obtain a better baseline for comparison than a random guess, we also calculated the probability gains for two simple reference strategies (Tejedor *et al.* 2009). They just focus on the temporal sequence without taking into account

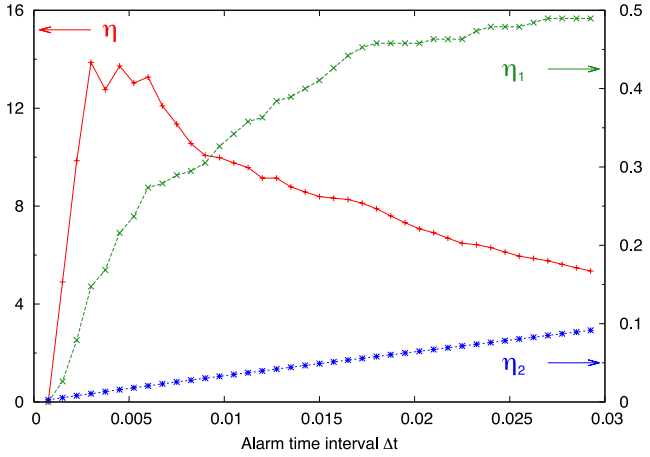

Figure 6. Results of the temporal forecast procedure for target events with an area larger that $A_{\min} = 1.6 \times 10^4$. We plot $\eta_1 = N_{\text{predicted}}/N_{\text{total}}$, $\eta_2 = T_{\text{alarm}}/T_{\text{total}}$ and $\eta = \eta_1/\eta_2$ as a function of the alarm time interval Δt. See text for description.

the internal mechanisms that evolve in the system. One consists in waiting some time τ_1 after each event and then declare an alarm which will be active until the next event. In the other strategy, the alarm is declared for some time interval τ_2 just after each event. If large events in the model are more periodic or more clustered than a Poisson process, these simple strategies will, respectively, yield better results than a random guess. Trying different values of τ_1 and τ_2 we obtained probability gains that are always below $\sim$2, much smaller than the obtained values for the forecast algorithm proposed here. Our results thus show that the assumed knowledge of the strain state of the system, and the identification of precursor chains is sufficient to make some statistically significant forecast about the time of occurrence of future events of the model, whose size and location were known in advance due to the analysis of the strain configuration discussed in Section 4.1. This is the message we want to convey on this respect.

Some further comments are in order here. Firstly, the skill of this forecasting method can be evaluated with other measures. For example, we can use the gambling score proposed by Zhuang (2010) and applied by Zechar & Zhuang (2010), where they quantify the performance of earthquake forecasts with reputation points. We also applied this approach using a Poisson distribution as a reference model and obtained that the change in reputation is optimized around 1100 for the same value of Δt found in Fig. 6.

Secondly, it is worth noting that we observe that large target events are better predictable, as it has been noted in other statistical physics models, such as Hainzl *et al.* (2000) and Caruso & Kantz (2011).

Thirdly, the increased likelihood for a large event to occur after some typical activity pattern must be considered as a purely phenomenological observation. The physical origin of this effect is not obvious. However, Jagla (2011) systematically addressed the effect of small perturbations on the kind of model we use, and found that there is a well-defined increase in seismic activity during some characteristic time following the perturbation. This is precisely the effect we rely on to construct our temporal forecast scheme.

In actual and simulated seismicity, considerable variability has been observed in the occurrence rates of foreshock sequences (Shaw *et al.* 1992; Hainzl *et al.* 2000; Scholz 2002, and references therein). Also in our model it is observed that the precursor activity before large events may not exist at all, meaning that the prediction algorithm will certainly miss the precise time of occurrence of some large events (though not its size and spatial location).

The last comment points to the strength of the present protocol: many chains occur all across the system as a function of time. However, it is the combination of the precursor information with that of the highly stressed regions what reduces the number of false alarms launched, then making this protocol of potential practical utility. We believe that this is a key point of the present procedure that combines the two methods to predict real earthquakes described in Section 2.

5 SUMMARY AND CONCLUSIONS

In this paper, we have analysed the performance of a forecast protocol in the context of a statistical physics model of seismicity. The model is a modification of the one proposed by Olami *et al.* (1992) to describe in very simple terms the sliding of tectonic plates in a single planar fault scenario. The modified model incorporates relaxation effects in the plates as a fundamental ingredient (Jagla 2010; Jagla & Kolton 2010).

The forecast procedure is based on the assumed knowledge of the local mechanical state of the plates at every moment, and in the determination of particular sequences of events, that we called precursor chains. The results obtained indicate that this information is sufficient to make sensible statements about the spatial location of forthcoming large events and in a lesser extent about their time of occurrence. On one side, the direct analysis of deformation of the plate at a given time allows to identify patches with high slip deficit where large 'delays' of the plate are occurring with respect to the long-term displacement rate. These overdue regions are systematically observed to be those that eventually unlock and generate the large events in the system. In this sense, the magnitude and spatial location of the large events can be predicted with a great degree of confidence. With respect to the prediction of time of occurrence, we have observed that in a fraction of the cases, large events are anticipated by some typical precursor activity that can be used to trigger an alarm for an imminent event. To quantify the temporal forecast efficiency of the alarm-based protocol, we have used the dimensionless ratio η as the density of target events during periods of alarm, divided by this density at all times (known as probability gain). It is clear that we have to aim to the highest possible value of η to obtain the best performance forecast algorithm. We observed that the alarm time interval Δt can be properly adjusted to maximize η, which for our present simulating parameters reaches values up to 14. On one hand, it is not obvious *a priori* what the highest value of η is that can be obtained with an optimized forecast protocol. On the other hand, on a practical perspective it is not clear either what the necessary η value is in order to have a practically useful forecast algorithm. Further work would be helpful along this direction. In any case, the results we have obtained with the present numerical model suggest that practical efforts to predict earthquakes must combine the two methods that have been considered as separate alternatives until present, namely, the determination of overdue regions in which large arrangements are likely to occur in some undetermined moment, and the search of precursor patterns within the overdue regions, that may likely tell when the large earthquake will be triggered.

Usually, forecast procedures in statistical physics models of seismicity are based on the magnitude, epicentre and occurrence time of events (e.g. Shaw *et al.* 1992; Hainzl *et al.* 2000; González *et al.* 2005, 2006; Tejedor *et al.* 2009; Caruso & Kantz 2011). Here, we

call for the need to complement these data with additional information that takes into account the elastic state of the system. Along this direction, Ramos (2010) analysed the correlation between the time-series of large events and the average stress of the modelled fault and its standard deviation in a modified version of the OFC model, and Anghel *et al.* (2004) studied the spatial modes of surface deformations in a geophysical model of the central San Andreas Fault. Nevertheless, in both cases they have focused on predicting the time of occurrence of large events. To our knowledge, our prediction protocol is the first that addresses not only the temporal occurrence, but also the spatial extent of future large events in a prospective manner.

There is a number of issues that we did not address in this paper, and that can potentially improve the results we have presented. Our model does not incorporate elastic interactions in a realistic, long-range way, but only between nearest neighbour blocks. It also disregards the possible effect of inertia of the blocks. Both facts can have an influence on the unrealistic feature of the model that large stress drops are many times 'decomposed' in a series of smaller events, in which none of them carries the large majority of stress drop, contrary to what happens in actual seismicity. Another important question is related with the fact that the model is supposed to describe seismicity in a single planar fault. In the best case, this can potentially have some relevance for the seismicity of subduction regions, where the assumption of a single fault may be justified. How the present results can be generalized to a context of multiple faults in a complicated geographical context is a totally unexplored issue at present.

ACKNOWLEDGEMENTS

This research was financially supported by Consejo Nacional de Investigaciones Científicas y Técnicas (CONICET), Argentina. Partial support from grant PIP/112-2009-0100051 (CONICET, Argentina) is also acknowledged.

REFERENCES

Anghel, M., Ben-Zion, Y. & Rico-Martinez, R., 2004. Dynamical system analysis and forecasting of deformation produced by an earthquake fault, *Pure appl. Geophys.,* **161**(9–10), 2023–2051.

Aragón, L.E., Jagla, E.A. & Rosso, A., 2012. Seismic cycles, size of the largest events, and the avalanche size distribution in a model of seismicity, *Phys. Rev. E,* **85,** doi:10.1103/PhysRevE.85.046112.

Baiesi, M., 2006. Scaling and precursor motifs in earthquake networks, *Physica A,* **360**(2), 534–542.

Baiesi, M. & Paczuski, M., 2004. Scale-free networks of earthquakes and aftershocks, *Phys. Rev. E,* **69,** doi:10.1103/PhysRevE.69.066106.

Boffetta, G., Cencini, M., Falcioni, M. & Vulpiani, A., 2002. Predictability: a way to characterize complexity, *Phys. Rep.,* **356**(6), 367–474.

Burridge, R. & Knopoff, L., 1967. Model and theoretical seismicity, *Bull. seism. Soc. Am.,* **57,** 341–371.

Carlson, J.M., Langer, J.S. & Shaw, B.E., 1994. Dynamics of earthquake faults, *Rev. Mod. Phys.,* **66**(2), 657–670.

Caruso, F. & Kantz, H., 2011. Prediction of extreme events in the OFC model on a small world network, *Eur. Phys. J. B,* **79,** 7–11.

Crampin, S., 2012. Comment on the report 'Operational earthquake forecasting' by the International Commission on Earthquake Forecasting for Civil Protection, *Ann. Geophys.,* **54**(May), 315–391.

Crampin, S., Gao, Y. & Peacock, S., 2008. Stress-forecasting (not predicting) earthquakes: a pradigm shift? *Geology,* **36,** 427–430.

Eberhard, D.A.J., Zechar, J.D. & Wiemer, S., 2012. A prospective earthquake forecast experiment in the western Pacific, *Geophys. J. Int.,* **190**(3), 1579–1592.

Eneva, M. & Ben-Zion, Y., 1997. Application of pattern recognition techniques to earthquake catalogs generated by model of segmented fault systems in three-dimensional elastic solids, *J. geophys. Res.,* **102**(B11), 24 513–24 528.

Geller, R., Jackson, D., Kagan, Y. & Mulargia, F., 1997. Earthquakes cannot be predicted, *Science,* **275**(5306), 1616.

González, Á., Gómez, J. & Pacheco, A., 2005. The occupation of a box as a toy model for the seismic cycle of a fault, *Am. J. Phys.,* **73**(10), 946–952.

González, Á., Gómez, J. & Pacheco, A., 2006. Erratum: 'The occupation of a box as a toy model for the seismic cycle of a fault', *Am. J. Phys.,* **75**(3), 286.

Grassberger, P., 1994. Efficient large-scale simulations of a uniformly driven system, *Phys. Rev. E,* **49,** 2436–2444.

Hainzl, S., Zöller, G., Kurths, J. & Zschau, J., 2000. Seismic quiescence as an indicator for large earthquakes in a system of self-organized criticality, *Geophys. Res. Lett.,* **27**(5), 597–600.

Helmstetter, A., Hergarten, S. & Sornette, D., 2004. Properties of foreshocks and aftershocks of the nonconservative self-organized critical Olami-Feder-Christensen model, *Phys. Rev. E,* **70,** 046120, doi:10.1103/PhysRevE.70.046120.

Hergarten, S., 2002. *Self-Organized Criticality in Earth Systems,* Springer-Verlag.

Hough, S., 2010. *Predicting the Unpredictable: The Tumultuous Science of Earthquake Prediction,* Princeton Univ. Press.

Jagla, E.A., 2010. Realistic spatial and temporal earthquake distributions in a modified Olami-Feder-Christiensen model, *Phys. Rev. E,* **81,** 046117, doi: 10.1103/PhysRevE.81.046117.

Jagla, E.A., 2011. Delayed dynamic triggering of earthquakes: evidence from a statistical model of seismicity, *Europhys. Lett.,* **93,** 19001, doi:10.1209/0295-5075/93/19001.

Jagla, E.A. & Kolton, A.B., 2010. A mechanism for spatial and temporal earthquake clustering, *J. geophys. Res.,* **115**(B5), 1–13.

Jordan, T. & Jones, L., 2011. Reply to 'A second opinion on "Operational earthquake forecasting: some thoughts on why and how," by Thomas H. Jordan and Lucile M. Jones,' by Stuart Crampin, *Seismol. Res. Lett.,* **82**(2), 231–232.

Jordan, T. *et al.*, 2011. Operational earthquake forecasting. State of knowledge and guidelines for utilization, *Ann. Geophys.,* **54**(4), 315–391.

Kanamori, H., 1981. The nature of seismicity patterns before large earthquakes, in *Earthquake Prediction: An International Review,* Maurice Ewing Ser., pp. 1–19, eds Simpson, W. & Richards, G., American Geophysical Union.

Kawamura, H., Hatano, T., Kato, N., Biswas, S. & Chakrabarti, B.K., 2012. Statistical physics of fracture, friction, and earthquakes, *Rev. Mod. Phys.,* **84**(2), 839–884.

Keilis-Borok, V., Shebalin, P., Gabrielov, A. & Turcotte, D., 2004. Reverse tracing of short-term earthquake precursors, *Phys. Earth planet. Inter.,* **145**(1–4), 75–85.

Kossobokov, V.G., 2006. Quantitative earthquake prediction on global and regional scales, *AIP Conf. Proc.,* **825**(1), 32–50.

Li, J.Z., Bai, Z.Q., Chen, W.S., Xia, Y.Q., Liu, Y.R. & Ren, Z.Q., 2003. Strong earthquakes can be predicted: a multidisciplinary method for strong earthquake prediction, *Nat. Hazards Earth Syst. Sci.,* **3**(6), 703–712.

Lippiello, E., Marzocchi, W., de Arcangelis, L. & Godano, C., 2012. Spatial organization of foreshocks as a tool to forecast large earthquakes, *Sci. Rep.,* **2**(846), doi:10.1038/srep00846.

Madariaga, R., Métois, M., Vigny, C. & Campos, J., 2010. Central Chile finally breaks, *Science,* **328**(5975), 181–182.

Molchan, G. & Romashkova, L., 2011. Gambling scores in earthquake prediction analysis, *Geophys. J. Int.,* **184**(3), 1445–1454.

Nanjo, K.Z., 2010. Earthquake forecast models for Italy based on the RI algorithm, *Ann. Geophys.,* **53,** 117–127.

Nature Debates, 1999. Is the reliable prediction of indiviual earthquakes a realistic scientific goal? Available at: http://www.nature.com/nature/debates/earthquake/equake_frameset.html (last accessed 1 October 2012).

Nishimura, T., Hirasawa, T., Miyazaki, S., Sagiya, T., Tada, T., Miura, S. & Tanaka, K., 2004. Temporal change of interplate coupling in northeastern Japan during 1995–2002 estimated from continuous GPS observations, *Geophys. J. Int.,* **157**(2), 901–916.

Olami, Z., Feder, H.J.S. & Christensen, K., 1992. Self-organized criticality in a continuous, nonconservative cellular automaton modeling earthquakes, *Phys. Rev. Lett.,* **68,** 1244–1247.

Omori, F., 1894. On the aftershocks of earthquakes, *J. Coll. Sci. Imp. Univ. Tokyo,* **7,** 111–200.

Panakkat, A. & Adeli, H., 2008. Recent efforts in earthquake prediction (1990–2007), *Nat. Hazards Rev.,* **9**(2), 70–80.

Pelletier, J., 2000. Spring-block models of seismicity: review and analysis of a structurally heterogeneous model coupled to a viscous asthenosphere, in *GeoComplexity and the Physics of Earthquakes,* Geophysical Monograph Series, pp. 27–42, eds Rundle, J.B. & Turcotte, D.L., American Geophysical Union.

Ramos, O., 2010. Criticality in earthquakes. Good or bad for prediction? *Tectonophysics,* **485**(1–4), 321–326.

Reid, H.F., 1911. Elastic rebound theory, *Univ. Calif. Publ., Bull. Dept. Geol. Sci.,* **6,** 413–433.

Rhoades, D.A., 2010. Lessons and questions from thirty years of testing the precursory swarm hypothesis, *Pure appl. Geophys.,* **167**(6–7), 629–644.

Ruegg, J.C. *et al.*, 2009. Interseismic strain accumulation measured by GPS in the seismic gap between Constitución and Concepción in Chile, *Phys. Earth planet. Inter.,* **175**(1–2), 78–85.

Scholz, C.H., 2002. *The Mechanics of Earthquakes and Faulting,* Cambridge Univ. Press.

Shaw, B.E., Carlson, J.M. & Langer, J.S., 1992. Patterns of seismic activity preceding large earthquakes, *J. geophys. Res.,* **97**(B1), 479–488.

Shcherbakov, R., Turcotte, D.L., Rundle, J.B., Tiampo, K.F. & Holliday, J.R., 2010. Forecasting the locations of future large earthquakes: an analysis and verification, *Pure appl. Geophys.,* **167,** 743–749.

Shebalin, P., 2006. Increased correlation range of seismicity before large events manifested by earthquake chains, *Tectonophysics,* **424**(3–4), 335–349.

Shebalin, P., Keilis-Borok, V., Gabrielov, A., Zaliapin, I. & Turcotte, D., 2006. Short-term earthquake prediction by reverse analysis of lithosphere dynamics, *Tectonophysics,* **413**(1–2), 63–75.

Sornette, D. & Werner, M., 2009. Statistical physics approaches to seismicity, in *Complexity in Earthquakes, Tsunamis, and Volcanoes, and Forecast,* pp. 7872–7891, ed. Meyers, R., Encyclopedia of Complexity and Systems Science, Springer.

Tejedor, A., Gómez, J.B. & Pacheco, A.F., 2009. Prediction of stasis and crisis in the Bak-Sneppen model, *Phys. Lett. A,* **373,** 4077–4081.

Wyss, M., 1997. Cannot earthquakes be predicted? *Science,* **278**(5337), 487–490.

Wyss, M., Shimazaki, K. & Ito, A., 1999. Seismicity patterns their statistical significance and physical meaning, *Pure appl. Geophys.,* **155,** 203–205.

Zechar, J. & Jordan, T., 2008. Testing alarm-based earthquake predictions, *Geophys. J. Int.,* **172,** 715–724.

Zechar, J.D. & Zhuang, J., 2010. Risk and return: evaluating Reverse Tracing of Precursors earthquake predictions, *Geophys. J. Int.,* **182**(3), 1319–1326.

Zhuang, J., 2010. Gambling scores for earthquake predictions and forecasts, *Geophys. J. Int.,* **181**(1), 382–390.

APPENDIX A: DETERMINATION OF THE STRESS FIELD FROM THE ACTIVITY HISTORY

The prediction procedure analysed in this paper assumes the full knowledge of the strain state of the system, contained in the function w_i. The direct information of the strain state in actual faults would be very difficult to achieve, although, as we have mentioned, modern technologies can help on this. However, we will show here that the function w_i can be determined in principle if we have access to the full detailed history of earthquake activity. In our model, this corresponds to know the spatial displacement h_i generated for every event that occurred in the past.

To obtain an analytical solution for the strain field at all times in a region Ω, we reconsider the evolution equation for the variables u_i (eq. 2). That equation is valid only in the times in between avalanches. To write down an equation that is valid at any time, we introduce a new term $H(\vec{r},t)$ which makes reference to the history of the local slips caused by previous events, namely:

$$\frac{\partial}{\partial t}u(\vec{r},t) = R(\nabla^2 u) + k_1 V + H(\vec{r},t), \tag{A1}$$

where $H(\vec{r},t)$ gathers information on the activity in the system prior to the present time t, and where for practical purposes we have passed from the discrete to a continuous-space description. The function $H(\vec{r},t)$ is written as

$$H(\vec{r},t) = -\sum_{j:(t_j<t)} \delta(t-t_j)\Delta u^j(\vec{r}), \tag{A2}$$

where t_j is the time of occurrence of event j, that produces a spatial stress drop distribution given by the function $\Delta u^j(\vec{r})$. The seismic moment $S(t_j)$ of the event can be calculated from the $\Delta u^j(\vec{r})$ function as

$$S(t_j) = \int_\Omega \mathrm{d}\vec{r}\,\Delta u^j(\vec{r}). \tag{A3}$$

Using Green's functions methods to solve differential equations, an analytical solution for the stress field may be obtained in the form

$$u(\vec{r},t) = k_1 V t - \sum_{j:(t_j<t)} g_j(\vec{r}, t-t_j), \tag{A4}$$

$$g_j(\vec{r},t-t_j) = \frac{1}{4\pi}\int_\Omega \mathrm{d}\vec{r'}\frac{\Delta u^j(\vec{r'})}{(t-t_j)}\exp\left(\frac{-|\vec{r}-\vec{r'}|}{4R(t-t_j)}\right). \tag{A5}$$

These equations solve in principle the problem: from these equations the strain distribution in the system can be evaluated if we have a detailed record of the stress drop function Δu for all events that occur before the present time (and know also the correct value of R). From a practical point of view, we need to know this function only for events that occurred, with respect to the space and time of interest, at spatial distance Δx and a time Δt for which $\Delta x^2/R\Delta t$ is not much smaller than one, because otherwise its contribution to the previous integral is vanishingly small.

In practice, it is difficult to compute the function $g_j(\vec{r},t-t_j)$. Nevertheless, if we consider the approximation that events occur locally in their epicentres $\vec{r}_0$ ($\Delta u^j(\vec{r}) = S(t_j)\delta(\vec{r}-\vec{r}_0)$) the function g_j can be directly obtained from the seismic moment at time t_j and its epicentre. Within this approximation, the stress field may be computed from the data that are usually measured, namely, the epicentre and magnitude of an event, as

$$u(\vec{r},t) = k_1 V t - \sum_{j:(t_j<t)} \frac{S(t_j)}{(t-t_j)}\exp\left(\frac{-|\vec{r}-\vec{r}_0|}{4R(t-t_j)}\right). \tag{A6}$$

Summarizing this part, we have shown that the stress field u_i, can be reconstructed if we have access to a detailed history of the activity in the system. More precisely, we should know, for each event j, occurred at time t_j, the local stress drop $\Delta u^j(\vec{r})$. We should also know the relaxation parameter R, which is supposed to be uniform throughout the region of interest. To determine if we should use the exact form (A4), or if we can use the much simpler approximation given by (A6) will require further analysis for each particular situation.